Chapter 14
Three-Dimensional Geometric Morphometrics in Paleoecology

Sabrina C. Curran

Abstract Quantification and analysis of shape is an important component of many paleoecological studies. Geometric morphometrics is a powerful shape analysis tool that allows its user to compare entire regions of morphology, visualize shape differences between groups, and create visualizations based on real data. This method is rapidly becoming the standard for data collection and analysis in many fields such as anthropology, biology, ecology, forensics, paleontology, and zoology. Here, the basic procedures of geometric morphometrics are reviewed and a case study on the ecomorphology of the cervid calcaneus is provided to illustrate how geometric morphometrics can be used in paleoecological studies.

Keywords Shape analysis • Surface • Outline • Landmark • Ecomorphology • Multivariate analysis • Artiodactyla • Cervidae

Introduction

Identifying and interpreting differences in morphology is a central theme to many paleoecological studies, including palynology (Mander and Punyasena 2018), phytolith studies (Strömberg et al. 2018), macrobotanical analysis (Peppe et al. 2018), dental mesowear and microwear (Green and Croft 2018), functional morphology (Dunn 2018; Evans and Pineda-Munoz 2018), and ecomorphology (Barr 2018). This chapter reviews three-dimensional (3D) geometric morphometrics methods currently being employed in paleoecological contexts.

Geometric morphometrics (GM) is rapidly becoming the standard method in biological and paleontological studies of morphology. It is widely used in ecological studies of masticatory behavior and locomotor behavior (e.g., Aguilar-Medrano 2017; Fernández et al. 2016; Ritzman et al. 2016; Taylor et al. 2016; van Heteran et al. 2016). Operating with a robust definition of shape and resting on a firm statistical foundation, GM methods are appropriate for a wide variety of shape-related questions, many of which had existed as qualitative descriptions previously. GM allows researchers to provide a high-resolution description of shape, analyze the entirety of an anatomical feature as a unit, take into account the 3D structure of shape, visualize shape differences, and even create hypothetical shapes based on actual data. Although not appropriate for every paleoecological study, GM is a powerful tool for shape-related research, especially for contexts wherein the researcher is interested in complex morphology.

It should be noted that there are many more shape analysis methods than are covered by this chapter, such as Elliptical Fourier Analysis (Slater et al. 2010; Panagiotopoulou 2009), Eigenshape Analysis (MacLeod 1999; Sheets et al. 2006), joint-surface angular interfaces (Tocheri et al. 2008, 2011), dental topographic analysis (Evans and Fortelius 2008; Eronen et al. 2010; Smits and Evans 2012), and superquadrics (Sommer et al. 2006). The method covered here (Geometric Morphometrics) was selected due to its ubiquity and flexibility. Although this method can be applied to the morphology of almost any set of specimens that have homologous features, I will focus on biological specimens and specifically skeletal elements (generally referred to as "objects" here) and applications in ecological functional morphology (ecomorphology). A case study on Pleistocene Eurasian Cervidae (deer and relatives) ecomorphology will be used to illustrate how one can use geometric morphometrics in paleoecological research.

S. C. Curran (✉)
Department of Sociology and Anthropology, Ohio University,
124 Bentley Annex, Athens, OH, USA
e-mail: currans@ohio.edu

D. A. Croft et al. (eds.), *Methods in Paleoecology: Reconstructing Cenozoic Terrestrial Environments and Ecological Communities*, Vertebrate Paleobiology and Paleoanthropology, https://doi.org/10.1007/978-3-319-94265-0_14

Historical and Theorectical Background

What we still refer to as solid geometry was mostly eloquently articulated by Euclid of Alexandria in the third century BCE in the *Elements*, which are considered some of the most influential mathematical texts of all time (Boyer 1991). Euclidean geometry defines the space in which most of the techniques of quantitative shape analysis work and form the basis of how we think about shape to this day. Quantification of Euclidean dimensions (length, width, depth, etc.) dominate studies of functional morphology. Such measures (referred to as traditional morphometrics) are useful in describing shape variation; however, they are difficult to apply to very complex shapes such as joint surfaces. Analyses using traditional morphometrics are further complicated by the effects of body size differences, which can be great in biological studies. Geometric morphometrics, which is described in detail below, is well-suited for addressing these issues in the analysis of complex shapes.

Although the origins of GM can be traced back to 1977 with David Kendall's work on stone circles (or even conceptually back to D'Arcy Thompson's deformation grids in 1917), the foundational principles set forth by Bookstein (1978) were worked out in a series of workshops and conferences in the 1980s and 1990s. These meetings resulted in what are referred to as the "color books", for each published proceedings or text has a dominant cover color (Red: Bookstein et al. 1985; Blue: Rohlf and Bookstein 1990; Orange: Bookstein 1991; Black: Marcus et al. 1993; White: Marcus et al. 1996; and later, Green: Zelditch et al. 2004; Yellow: Cardini and Loy 2013). Over the past twenty-eight years, GM methodology has evolved from a "revolution" (Rohlf and Marcus 1993), to a "synthesis" (Bookstein 1996), to a "paradigm" (Adams et al. 2013).

Geometric morphometrics offers a different way of evaluating the shape of an object than is afforded by traditional morphometric studies (Mitteroecker and Gunz 2009; Baab et al. 2012; Adams et al. 2013; Cooke and Terhune 2015; McNulty and Vinyard 2015). In GM, data are collected as two-dimensional or three-dimensional coordinates across a region of interest that contain all of the information that one would describe qualitatively and/or measure with traditional methods. For example, say we are analyzing the shape of hominin crania when viewed from posterior. We could describe the cranium of *Australopithecus* as being somewhat bell-shaped, *Homo neanderthalensis* as 'en bombe' or oval-shaped, and *Homo sapiens* as being shaped like the end of a loaf of bread. To quantify such shapes with traditional morphometrics, we could take a series of measurements from the posterior cranium, such as cranial height (the distance between osteometric points basion and bregma) or cranial breadth (the distance between left and right euryon) and create ratios from them. However, we would still be missing information about the regions between those measurements including the overall curvature of the cranial vault, which can provide a more detailed understanding of cranial morphology and facilitate comparisons between taxa. With GM, we could analyze the outline of the cranium (from a two-dimensional photograph) or the entire surface of the cranium (from three-dimensional scans). Not only would we maximize retention of information about the overall shape of the cranium throughout the analysis, but we would also be able to visualize the differences found in the collected data since we can apply vector transformations to the original data, which is much more difficult to do with traditional morphometrics. Thus, GM allows morphologists to quantify features that are traditionally described qualitatively. Further, we can even create hypothetical specimens based on the digitized data. For these reasons and others, geometric morphometrics is a powerful tool for the morphologist. In paleoecology, shape analysis is important for studies of both ecological functional morphology (ecomorphology) and taxonomy (used in many ecological methods).

In GM, the shape of an object is digitized as a series of 2D or 3D landmark coordinates that are superimposed in a single coordinate system (described in detail below) for analysis. The resulting coordinates (called Procrustes coordinates) are the raw data that can be analyzed using standard multivariate methods used in the study of shape. However, unlike traditional morphometric data, GM analyses maintain all the interrelationships of the original coordinates are maintained, including interlandmark distance and angles (Slice 2007). Thus, the variation in shape can easily be visualized and hypothetical specimens can be created. For example, in a study of variation in cervid femoral head shape as it relates to locomotor behavior in different habitats (Curran et al. 2016), the average femoral head shape for cervids in different habitats or the shape changes along principal components axes can be visualized (Fig. 14.1). Furthermore, one can explore hypothetical femoral head shapes in multivariate space based on the specimens in the space (such as the average specimen in the center of Fig. 14.1) allowing researchers to ask questions about their data that may not have been possible before.

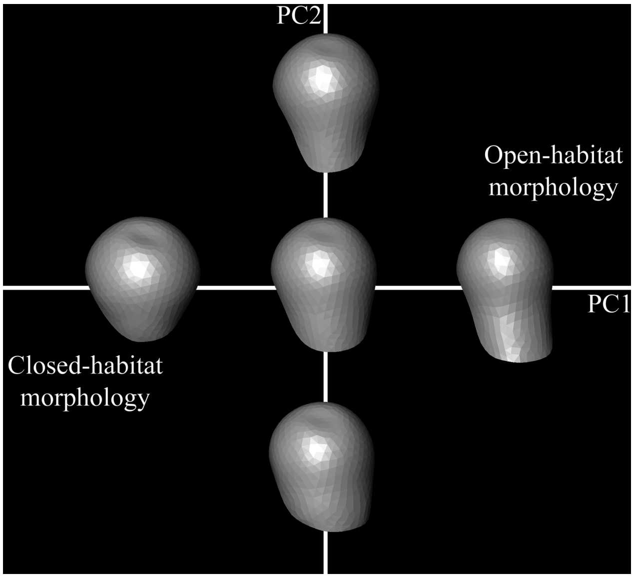

Fig. 14.1 Visualizations of cervid femoral head shape (in superior view) differences along PC1 (68% of variation) and PC2 (26% of variation), with the average specimen at the origin. Open-adapted cervids are distributed along the positive sides of PCs 1 and 2, while closed-adapted cervids are along the negative sides of the axes

Methodology

Geometric morphometrics (GM) analysis begins with the selection and digitization of landmarks, which are points that are homologous, or at least operationally homologous, between specimens. For semilandmark analysis, curves or surfaces of a region are considered homologous when anchored by landmarks (Bookstein 1991, 1996/1997; Gunz et al. 2005) and are digitized as a series of coordinates across a region. Selection of landmarks is important because they must be present in all specimens in the analysis and provide sufficient coverage of the anatomical region in question. It should be noted that these landmarks are homologous in a geometrical rather than biological sense (that is, the landmark location, itself, is likely not the unit of selection, but rather a part of the biologically homologous region; Gunz et al. 2005). Further, not all landmarks are considered to be equal. Ideally, landmarks are placed at discrete anatomical loci, such as the intersection of cranial sutures or foramina (Bookstein 1991). Such landmarks are called Type I and carry the highest repeatability. For example, a Type I landmark on the human skull, the craniometric point 'nasion' is defined as the intersection of the frontal bone and the two nasal bones. Barring pathology or damage, this landmark is easy to locate and present on all human skulls. Type II landmarks are those placed on anatomical features that include tips of protuberances, bases of pits, and maxima of curved features, such as the tip of the (unworn) canine (Bookstein 1991). Type III landmarks are commonly used as the end points of conventional (caliper) measurements, such as lengths and widths. The craniometric point 'euryon', for example, is found on each side of the cranium to record its greatest breadth. Type III landmarks are defined in reference to other features are the least repeatable and perhaps the least likely to be equivalent among individuals. In landmark-based GM analyses, it is best to use as many Type I and II landmarks as possible.

If the region of interest is devoid of landmarks, as is the case for joint surfaces and other smooth features such as much of the human cranial vault, then semilandmark analyses may be used (Bookstein 1996/1997). Although the semilandmark coordinates are not necessarily homologous, the region of interest from which the data are collected (curve or surface) is considered homologous (Perez et al. 2006). Semilandmarks can be collected in a variety of ways. For a 2D analysis, points are usually digitized from an image using software (e.g., the tps suite by Rohlf (2015)). In 3D analyses, points are digitized either directly from a specimen using a MicroScribe (in Excel or visualized in real time using CAD software such as Rhinoceros®), or extracted from models created with a 3D scanning device (laser scanners, structured-light scanners, CT-scanners, etc.) or photogrammetry. With many of the data collection tools, coordinates will need to be extracted from digitized models using software such as Landmark Editor (Wiley et al. 2005) or several R packages (see below). Landmarks are generally selected as a starting and end points (minimally) along the feature and then semilandmarks are digitized from a curve or surface in between those landmarks. As with a landmark-based analysis, the number of landmarks on each specimen must be equal and thus the user either must specify a number of semilandmarks across the region of interest or resample (Curran 2012; Gunz et al. 2005; Harcourt-Smith et al. 2008) a surface or outline created from the digitized coordinates. Next, a sliding procedure is conducted on the collected coordinates wherein semilandmarks 'slide' along tangents to the curve or surface from which they are derived until all semilandmarks are in roughly homologous locations (Gunz and Mitteroecker 2013). This process starts with a reference or template specimen and is iteratively repeated based on a mean configuration. The resulting semilandmarks then are projected back down on to the original curve or surface of the target specimen (Gunz et al. 2005; Gunz and Mitteroecker 2013).

Once all landmarks or semilandmarks have been digitized for all specimens, their coordinates are submitted to a Generalized Procrustes Analysis (GPA). Specimens are typically digitized in slightly different orientations and positions, which will introduce differences in the coordinates that are irrelevant to the shape of the specimen. GPA superimposition removes this extraneous information about location, isometric size, and orientation.

To remove information about a specimen's digitized/scanned location, the centroid of each specimen configuration is moved in space to a common origin. A specimen's centroid is found by calculating the mean *x,* mean *y,* (and mean *z* for 3D analyses) coordinate of every point in its configuration (the "center of gravity" for all the landmarks; McNulty 2003, p. 61). Subtracting the specimen's mean *x* from all of its *x*-coordinates, the mean *y* from its *y*-coordinates, and the mean *z* from its *z*-coordinates translates the specimen to the origin; when applied to all specimens, this eliminates any differences between objects due to their location.

Especially important to the study of biological variation is that isometric size, which is often one of the greatest differences between specimens in traditional morphometric analyses (Falsetti et al. 1993; Jungers et al. 1995), can be removed as a confounding factor in the initial stages of the GPA, however, allometric shape variation still remains in the data (Klingenberg 2016). Landmark configurations are scaled isometrically by removing size differences among specimens by dividing each coordinate of a specimen by that specimen's centroid size, a measure of size that has no correlation to shape, by setting all configurations to a centroid size of one (Zelditch et al. 2004). Centroid size is calculated as the square root of the sum of squared distances of a specimen's landmarks to its centroid (Bookstein 1991; Dryden and Mardia 1998; Mitteroeker and Gunz 2009). It should be noted that with certain research questions it may be undesirable to remove size from an analysis (Klingenburg 2016) since size, itself, is an ecological variable. In fact, GM methods allow the researcher to parse out size and shape and examine them individually or in concert.

To remove information about a specimen's digitized/scanned orientation, coordinate configurations are rotated to minimize the distance between each specific landmark across all specimens. This is an iterative least-squares process in which sum-of-squared distances between each landmark are minimized (Slice 2005). In the first iteration, a mean configuration (reference configuration) of translated and scaled specimens is produced on to which all specimen configurations (target configurations) are then superimposed. A new mean configuration is then calculated and the process is repeated until further superimpositions produce negligible differences in distance minimization.

There are several software packages available to conduct a GPA (and other analyses), such as Morphologika (O'Higgins and Jones 2006), Morpheus (Slice 2002), MorphoJ (Klingenberg 2011), EVAN toolbox (EVAN Society, http://www.evan-society.org/), PAST (Hammer et al. 2001), and through R packages such as geomorph (Adams and Otarola-Castrillo 2013) and Morpho (Schlager 2017). Many of these are freely available through the Stony Brook morphometric website (http://life.bio.sunysb.edu/morph/), which is a useful starting point for GM studies in general. Consult Appendix 14.1 for other software packages.

Following a GPA, the objects are aligned to share a common coordinate system, which can be organized in a matrix or 3D array, and can be used as shape variables (Slice 2005), called Procrustes coordinates. These coordinates are the data that are submitted to multivariate analyses. For a 3D analysis, each *x, y, z* value for each landmark is input as a variable in future analyses (Cardini and Elton 2007; Cardini et al. 2015), thus (for example) a 3D configuration with 20 landmarks will have 60 variables for multivariate analyses. Here, a word of caution must be extended. Geometric morphometrics is a powerful method for analysis of shape differences; however, there are specific criteria that must be met for its use. In most studies of shape variance, including those based in traditional morphometrics, large sample sizes are desired. In the case of GM, large sample sizes are often necessary due to the large number of variables inherent to its methods This is particularly important if one is considering doing any multivariate analysis that involves matrix inversion, such as canonical variates analysis (described below). Further, the user should have a robust understanding of the assumptions in both geometric morphometrics (beyond the basics covered here-the reader is referred to Slice (2007) as a good starting point and to the "color" books listed above) and any multivariate analyses (Neff and Marcus 1980) they might use in order to avoid violating those assumptions and obtaining false results (the 'garbage in, garbage out' principle).

The following is an overview of some of the multivariate methods available, and it not meant to be exhaustive. GM is a rapidly growing field and these methods continue to be improved upon and new methods appear frequently. If you are interested in exploring the distribution of morphological variation in your sample, then principal components analysis (PCA) is a typical starting point, however, there is recent criticism of the use of this method in GM (Bookstein 2016, 2017b). Currently, PCA is used in two main applications in GM studies-data reduction and exploration. PCA recombines the original variables by rigidly rotating the data and creating new axes (the principal components, or PCs) that are mathematically uncorrelated (orthogonal) and which summarize sample variance in lower dimensionality. In doing so, the user now has fewer variables (the PCs, along which each specimen is scored), with the first PC summarizing the most variation in the sample, and each subsequent PC summarizing less and less. Typically, the majority of sample variance can be summarized in far fewer PCs than the number of original variables. The PCs are usually plotted against one another and the user then explores the distribution of specimens in the PC morphospace.

There are several methods available to explore the relationship between shape (e.g., Procrustes coordinates) and other variables such as sex, size, time, phylogeny, and ecological variables (e.g., temperature, precipitation, diet, trophic level, etc.). Multivariate regression and multiple multivariate regression can be used to test for correlations between one or more independent variables (such as those listed above) with several dependent variables (shape data; Frost et al. 2003; Klingenberg 2011; Cáceres et al. 2014). Partial Least-Squares (PLS; sometimes called 2-Block partial least-squares, 2B-PLS; Rohlf and Corti 2000) is commonly used to investigate covariance of two sets of data (for example, shape and environmental variables or two different shapes) without the assumption of one data set as a predictor variable (Monteiro et al. 2003; Colangelo et al. 2010; Piras et al. 2012; Cáceres et al. 2014; Meloro et al. 2014).

When the research goal is to classify unknown specimens into preselected (*a priori*) groups (sex, diet type, habitat, etc.) or to evaluate distinctness of *a priori* groups, linear discriminant analysis (LDA; two groups) or canonical variates analysis (CVA; multiple groups) is frequently used. Like PCA, CVA recombines the variables to create new variables (canonical variates, or CVs) to maximize variability between groups relative to variability within groups (Neff and Marcus 1980). However, unlike PCA, CVA is not a rigid rotation of the original data and distorts the original distribution of specimens by scaling distances between groups by within-group variance (Cooke and Terhune 2015). To proceed, the number of cases (specimens) should be greater than the number of variables (Kovarovic et al. 2011). In analyses with very high numbers of variables, the CVA will always show group separation, even if there is no biological reality to such a distribution (Mitteroecker and Bookstein 2011). However, group separation can be evaluated by the results of a cross-validation analysis and premutation tests (McNulty et al. 2006; Adams and Collyer 2015). Cross-validation removes one specimen or subsets of specimens, re-computes the CVA, and then classified the removed specimen(s) into a group. A likelihood of group membership (posterior probability) is calculated for each reclassified specimen and average correct reclassifications rates can be calculated for the training set (based on specimens of known group membership), which indicates how well the analysis will perform with unknown cases. One can also test the significance of group separation by using a permutation test based on known Mahalanobis squared distance (D^2; the squared distance between centroids, or the multivariate mean for each group) compared to randomly resampled (permuted) data between groups (Neff and Marcus 1980; McNulty et al. 2006; Curran 2009).

To overcome some of the short-comings of LDA and CVA, one can use a between-groups PCA (bgPCA), wherein group means, rather than individual specimens are used to calculate the PC axes and then all specimens are scored (and plotted) along those axes (Mitteroecker and Bookstein 2011; Gunz et al. 2012; Renaud et al. 2015; Cooke and Terhune 2015). Like CVA, a cross-validation can then be used to evaluate the correct reclassification rate for the bgPCA (Mitteroecker and Bookstein 2011).

Beyond providing a new way to collect and analyze shape data, GM also allows for visualizations of shape differences in a dataset, which is much more difficult to do with traditional morphometric data. One can visualize difference in landmark positions between specimens using thin-plate splines (TPS; Bookstein 1989; Zelditch et al. 2004), wire-frame models, and warped surfaces (Wiley et al. 2005; Klingenberg 2013). TPS visualizes differences between specimens (or averages of groups of specimens) using deformations on a grid (originally envisioned by Thompson in 1917). These deformations demonstrate regions where a uniform grid with plotted landmarks of a reference coordinate configuration would have to be deformed in order to keep the landmarks of a target configuration in the in the same locations on the grid (Bookstein 1989; Klingenberg 2013).

One could also visualize specific points in a morphospace that are not sampled by actual specimens, such as a group mean shape, or shape differences along a principal component axis. In the case study below, wire-frame visualizations were created for the extremes of a morphological feature under investigation. Using principal component scores from a PCA on the specimen's Procrustes coordinates, a single discriminant function can be produced to separate two predefined groups, such as comparing the calcanei between open habitat adapted cervids versus closed habitat adapted. The scores of each specimen along the discriminant function are regressed against the Procrustes coordinates for each specimen, which produces a vector of coefficients correlated with a grouping variable, such as habitat type (McNulty et al. 2006). When this vector is added to and subtracted from the consensus configuration (for the entire data set), it produces two new configurations that demonstrate the differences between the two extremes (such as "Open" and "Closed") along the vector (Frost et al. 2003). The vector can be multiplied in order to amplify shape differences, which allows for more obvious differentiation between the extremes by increasing the magnitude (but not direction) of the shape change. These changes can be visualized on wire-frame models for point data (the case for the study here) or across a surface for 3D scanned data. It should be noted that the only real data are the landmarks and semilandmarks; all transformations between them are interpolated (Klingenberg 2013).

Geometric morphometrics offers users a method for shape analysis that operates under a specific and clear definition of shape (the geometrical information that remains when the variation due to location, orientation, and scale are removed from an object (Slice 2007)), which enhances objectivity and replicability. Its basic theoretical principles (as described above) are well-established and the software (if not the hardware) to conduct GM analyses are free and becoming increasingly user-friendly. As such, GM methods are used ubiquitously throughout studies of anthropology, biology, and paleontology. Quantification and analysis of entire regions of shape and the maintenance of the interrelationships within the landmark configuration make geometric morphometrics a very appealing type of shape analysis, however, potential users should always ask if it is the appropriate method for their research question. While 2D analyses require only digital images, 3D analysis requires some type of digitizer (MicroScribe, laser or white-light scanner, CT-scanner, etc.), which can be expensive and processing of collected data can be time intensive. The benefit to the latter, of course, is that many biological features are three-dimensional and analysis in two-dimensions may result in loss of important information. However, with the limitations imposed by the necessity of large sample sizes and expensive equipment, in some cases a study using traditional morphometrics may be more appropriate, depending on one's question. In short, if your question can be answered with a few measurements, then do so. However, if you are interested in complex morphology with differences that can be quite subtle, geometric morphometrics may be a good fit for your research.

Case Study: Cervid Ecomorphology

The following case study is intended to give the reader a sense of the entire process of GM from data collection to results. This example is in no way meant to suggest the only manner in which to use this method, but instead to illustrate a specific question for which it is appropriate. Other examples of geometric morphometrics in ecomorphology and paleoecology include studies on reptiles and amphibians (Adams 2011; review in Kaliontzopoulou 2011), primates (White 2009; Cooke 2011), felids (Christiansen 2008; Walmsley et al. 2012), canids (Raia 2004), ursids (Figueirido et al. 2005; Figueirido and Soibelzon 2010; van Heteren et al. 2016), mustelids (Fabre et al. 2015; Bottom-Divet et al. 2017), voles (McGuire 2010), rodents (Cano et al. 2013; Morgan and Alvarez 2012), bovids (Forrest et al. 2018), and deer (Curran 2009, 2012, 2015), the latter of which will be illustrated below.

The deer family Cervidae, contains approximately 40 different species in five tribes (Gilbert et al. 2006). They live in a wide variety of habitats, including non-sand deserts (e.g., *Odocoileus hemionus*, mule deer), grasslands (e.g., *Ozotoceros bezoarticus*, pampas deer), tundra (e.g., *Rangifer tarandus*, reindeer/caribou), woodlands (e.g., *Caproelus caproelus*, roe deer), temperate forests (e.g., *Alces alces*, moose), and tropical forests (e.g., *Pudu puda*, pudu). In these different habitats, they must be able to escape predators and each habitat has different levels of vegetative complexity, topographic relief, and substrate firmness, which in turn require different forms of locomotion and predator-escape behaviors. For example, the reindeer/caribou inhabits open tundra and uses speed in flight and herding behavior to escape predators. Morphologically, having a stable joint surface with low risk of hip joint dislocation (at the cost of joint mobility) is of primary importance. Alternatively, the pudu occupies tropical forests and must move through complex vegetation and topographical relief when escaping predators. Joint stability is sacrificed for joint mobility in order to change direction quickly while fleeing. Adaptations for different locomotor strategies can be evaluated in joint surface morphology, whole bone shape, and in specific regions of skeletal elements (for further studies using GM on post-crania, see also Arias-Martorell et al. 2015; Bottom-Divet et al. 2017; Muñoz et al. 2017).

Ecomorphological studies have been conducted on the closely related family of Bovidae (antelope and relatives) using traditional morphometric methods. Notably, work by Kappelman (1988, 1991) demonstrated that several morphological aspects of the femur, especially femoral head shape and shape of the medial patellar margin correlate to different locomotor (habitat) adaptations. Subsequently, there were several ecomorphological studies of bovid post-crania (Plummer and Bishop 1994; Scott et al. 1999; DeGusta and Vrba 2003, 2005; Weinand 2007; Kovarovic and Andrews 2007; Plummer et al. 2008, 2015), although few started with explicit functional morphological hypotheses, with the recent exception of Barr's (2014, 2015, 2018) studies of the astragalus. Cervids have received much less attention than bovids in post-cranial ecomorphology studies, although several species were included by Kovarovic and Andrews (2007).

To fill this void, I collected three-dimensional landmark and semi-landmark data from across rear-limb skeletal elements in 33 extant and (minimally) five extinct species of deer

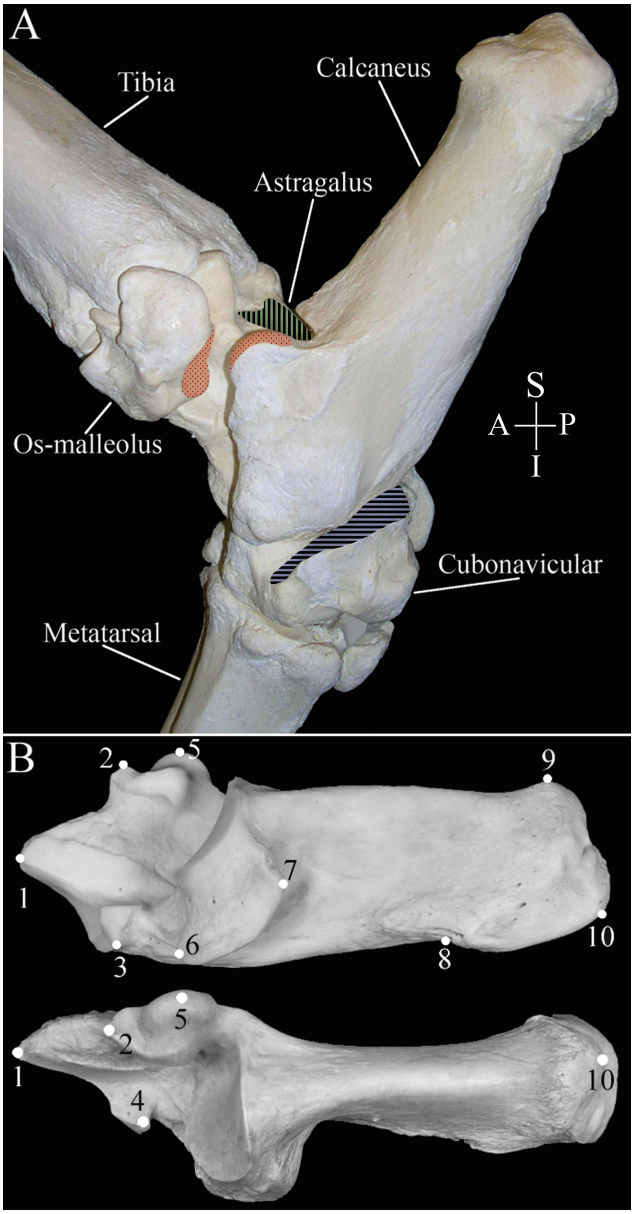

Fig. 14.2 A, Lateral view of left-side hock joint in articulation with skeletal elements labeled and joint surfaces highlighted: astragalus-calcaneus joint (vertical green and black stripes); os malleolus-calcaneus joint (pink and black stippling); cubonavicular-calcaneus joint (blue and black horizontal stripes). Orientation abbreviations: A, anterior; I, inferior; P, posterior; S, superior. B, Ten landmarks used in this study (numbered) on a right-side calcaneus in medial (top) and supero-anterior (bottom) views; both views are oriented with anterior to left

(many specimens were assigned to only Cervidae (gen. + sp. unknown) and exhibited a wide variety of sizes) to test the hypothesis that rear limb morphology reflects cervid locomotion in different habitats and substrates. Each extant species was assigned to a habitat type: Open (deserts, open grasslands, tundra), Intermediate Open (ecotones, tall grasslands, swamps), Intermediate Closed (woodlands/shrublands), and Closed (forests) (Curran 2009, 2012, 2015). Data were collected for 37 morphological features, but I will limit discussion here to the landmark-based geometric morphometric study of the calcaneus (n = 123 for extant specimens and n = 47 for fossil specimens) for illustrative purposes (Fig. 14.2).

In cervids, the calcaneus acts as a Class 1 lever, with the calcaneal-astragalar joint surface (vertically-striped area in Fig. 14.2A) as the fulcrum, the calcaneal body as the lever arm and the distal limb as the load arm. An increase in calcaneal length (approximated by landmarks 1 and 10 in Fig. 14.2B) increases the lever arm and thus increases the mechanical advantage of the contracting muscle that attaches onto the calcaneal tuber but reduces the speed of movement at the ankle. Conversely, a shorter calcaneus provides less power but a quicker movement. Cervids that utilize saltatorial locomotion (bounding leaps) to escape predators, which is an effective adaptive strategy common in more densely vegetated ecotones and closed habitats have longer calcanei than cervids that are cursorial in open habitats (Hildebrand 1985) with cervids that stott (leaping with all four feet contacting the substrate at the same time and mostly found in open mountainous regions) having the longest calcanei. The anterior process of the calcaneus articulates with three bones: anteriorly with the os malleolus (stippled region in Fig. 14.2A and landmark 5 in Fig. 14.2B), inferiorly with the cubonavicular (horizontally-striped region in Fig. 14.2A and between landmarks 1 and 3 in Fig. 14.2B), and at several places with the astragalus (vertically-striped region in Fig. 14.2A), but most especially on the sustentaculum tali (medial border demarked by landmarks 6 and 7 in Fig. 14.2B). Orientation of these joint surfaces affects the rest position of the calcaneus prior to lower limb extension, which, at the hock joint, is almost completely restricted to the parasagittal plane in cervids. The rest position of the calcaneus is hypothesized to determine how far the calcaneus moves along the astragalus when the gastrocnemius muscle is contracted (Fig. 14.3). If the calcaneus sits more vertically on the articulations with the cubonavicular and astragalus, then it moves a shorter distance, which allows for a quick but less powerful force to be generated. This morphology is associated with open-adapted cursors that increase speed by increasing the number of times the same foot strikes the ground per second (the pace cycle). A more horizontal rest position means that the calcaneus travels farther with the contraction of the gastrocnemius, which generates more power, but is slower. This morphology is associated with saltatorial runners that flee predators in a series of leaps that allow for maneuverability in more closed habitats.

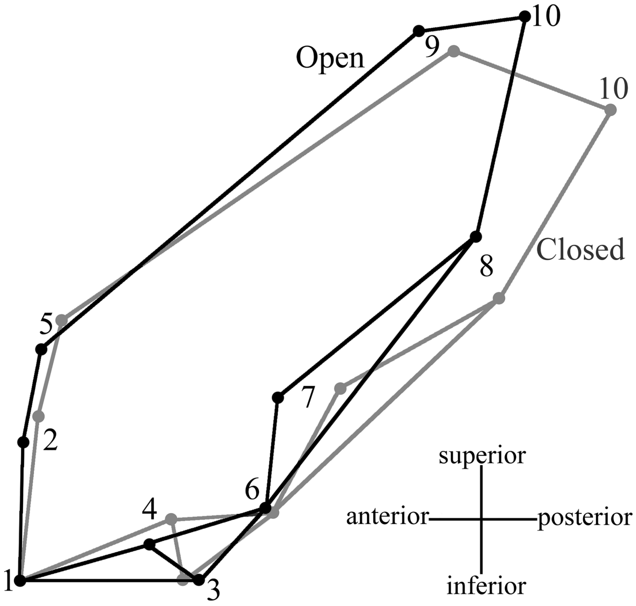

Fig. 14.3 Comparative rest position of the calcaneus of open-adapted (black wire-frame model) and closed-adapted (gray wire-frame model) cervids with landmarks numbered

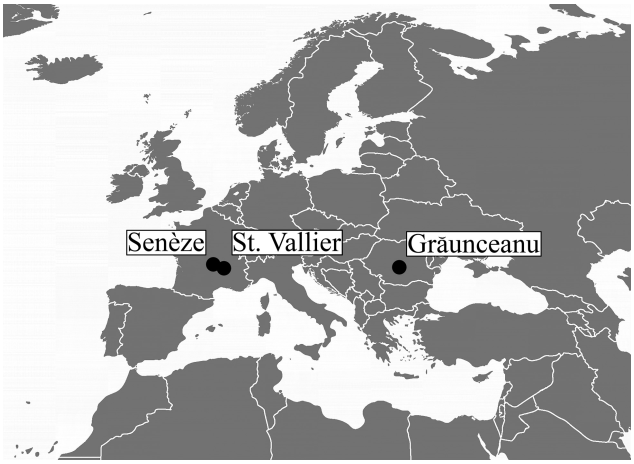

Fig. 14.4 Map of Pleistocene European fossil sites in this study

Once the comparative sample of extant cervid morphology is established, it can be used as a training set to classify cervid specimens of unknown locomotor behaviors (i.e., fossils). Here, this will be applied to cervids from three early Pleistocene sites (St. Vallier and Senèze in France and Grăunceanu in Romania; see Fig. 14.4), which contain several very large deer taxa, including *Cervalces* and *Eucladoceros* (Table 14.1). The three sites are slightly older (Nomade et al. 2014) than the first appearance of *Homo erectus* in Eurasia at Dmanisi, Georgia (maximally 1.85 Ma; Ferring et al. 2011), and contain some of the same cervid genera, however, specimens from Dmanisi were not available for this GM analysis. Using multiple habitat proxies (including macromammals (Gabunia et al. 2000; Palmqvist 2002; Lordkipanidze et al. 2007; Tappen et al. 2007; Hemmer et al. 2011), micromammals (Furió et al. 2010), herpetofauna (Blain et al. 2014), pollen (Gabunia et al. 2000; Messager et al. 2010a), phytoliths (Messager et al. 2010a, b), Dmanisi has been reconstructed as a variable but mostly arid, heterogeneous environment dominated by grasses, with more closed habitats such as woodlands and forests available nearby. The cervid taxa from Dmanisi include *Cervus* cf. *nestii* and *Eucladoceros* aff.

Table 14.1 Summary of fossil specimens in this study

Country	Site	Date	Cervids Present	*n*
Romania	Grăunceanu	Early Pleistocene	*Eucladoceros* sp.	17
France	St. Vallier	Early Pleistocene (2.4–2.1 Ma)	*Croizetoceros ramosus medius*	2
			Eucladoceros ctenoides vireti	3
			Cervidae (sp. + gen. unknown)	17
France	Senèze	Early Pleistocene (2.2–2.0 Ma)	*Alces* sp.	1
			Eucladoceros ctenoides senezensis	2
			Cervus sp.	1
			Cervidae (sp. + gen. unknown)	4
			Total	47

Table 14.2 Calcaneus landmarks (Cal LM) used in this study. Note: black dots in Figure 14.2B are landmarks that were not homologous and thus eliminated from the analysis

Landmark	Location description
1	Anterior point of cubonavicular articular surface
2	Anteroinferior point of lateral astragular articular surface
3	Anteroposterior point of cubonavicular articular surface
4	Superomedial point of anterior astragular articular surface
5	Anterosuperior point of os malleous articular surface
6	Inferomedial point of sustentacular tali
7	Superomedial point of sustentacular tali
8	Posteroinferior point of gactronemius enthesis
9	Anterosuperior point of calceneal tuber
10	Posterosuperior point of caleanal tuber

tegulensis, both of which are associated with “dense to open forests and shrub landscapes” (Lordkipanidze et al. 2007, Supplementary Table S2). To compare the reconstructed paleohabitat of Dmanisi to other European sites that do not contain hominins, GM ecomorphological analyses were conducted on cervid post-crania from St. Vallier, Senèze, and Grăunceanu.

Using a MicroScribe® MLX 3D point digitizer (http://www.3d-microscribe.com), *x, y,* and *z* coordinates for ten landmarks (Fig. 14.2B, Table 14.2) were directly uploaded into a spreadsheet (in this case, Excel). Once all data were collected on extant and extinct specimens, they were submitted to Morphologika (O’Higgins and Jones 2006) for Generalized Procrustes Analysis to translate them to the same origin, rotate them into the same orientation, and scale them to the same isometric size (as described above) (Fig. 14.3). The resulting Procrustes coordinates were then used in the following analysis.

The main goal of this study was to provide a new paleoecological proxy using cervid remains, which are often the most frequent taxa in Eurasian fossil assemblages. However, there are two main confounding factors (phylogenetic relatedness and body size) that need to be assessed before proceeding with the ecomorphological proxy analysis. Since cervids belong to the same family, they may share similar morphology due to common ancestry and this may bias the ecomorphological signal. To test for this, a phylogenetic signal was calculated in MorphoJ (Klingenberg 2011) by comparing the sum of branch lengths of a phylogenetic tree (=tree length) based on known phylogenetic relationships of the extant taxa (from 10kTrees; Arnold et al. 2012) and Procrustes coordinates (means for each species) to trees generated with randomly permuted tip taxa. The null hypothesis of no phylogenetic signal in the morphological data is rejected if 5% or more of the permuted tree lengths are shorter than the original (known lengths) tree. A significant p-value ($p \leq 0.05$) indicates a relationship between phylogeny and morphology. In this study, the *p*-value is 0.7105, a non-significant result.

To assess the relationship between allometric size differences (since isometric size has been removed from the data during the GPA) and calcaneal morphology, a multivariate linear regression (Monteiro 1999) was performed on body size of extant taxa and the Procrustes coordinates in the geomorph package for R (Adams and Otárola-Castillo

2013). Cervids vary in body size by two orders of magnitude (4.65 kg in *Pudu mephistophiles* to 513 kg in *Alces alces*; Novak 1999) and the metric data have to be log-transformed before any comparison can be made. To test for a relationship between size and shape before proceeding with the ecomorphological analysis, the natural log of centroid size (lnCS) was regressed against the natural log of body weight (lnBW) for extant cervids, resulting in $R^2 = 0.87$ and $p < 0.0001$. The lnCS of the Procrustes configurations was used as a proxy for body size in this analysis. Here, the correlation between lnCS and shape (Procrustes coordinates) was non-significant ($p = 0.3057$).

Once phylogeny and allometry are shown to not have a large impact on morphology (or adjustments are made for them if they do have an impact), Procrustes coordinates of the cervid calcaneus can be used as a paleohabitat proxy. Extant cervid specimens with a known habitat preference were used as a training set for canonical variates analysis (CVA) to categorize unknown (fossil) specimens into a habitat type. The habitat types used here are similar to those used in bovid ecomorphological studies, in that the continuum of habitats is broken down into the four categories described above (for details refer to Curran 2012). Since geometric morphometric analyses usually have a high number of variables (three for each Procrustes coordinate-the *x, y,* and *z* values in a 3D analysis) and since CVA requires more cases (specimens) than variables, data (including extant and extinct specimens) were first reduced using PCA. To avoid overfitting (making the analysis too specific to the extant training set and possibly reducing the ability to accurately assign fossil specimens to a habitat category; Kovarovic et al. 2011), the number of PCs used in further analyses was determined by the lowest number of PCs that returned the highest reclassification rate but retained at least 90% of the original sample variance (Sheets et al. 2006; Curran 2015). Here, 17 PCs, summarizing 94.56% of the total sample variance, were submitted to CVA.

Specimens in the CVA extant training sample were reclassified into their known habitat type with a mean accuracy rate of 61.7% using the cross-validation method and 79.1% with the resubstitution method (Table 14.3), results that are 2.47 and 3.16 times (respectively) better than by chance alone. To test if the habitat types were significantly different from each other, pair-wise non-parametric permutation tests were conducted on the centroids (group mean Procrustes coordinates) for each habitat type (after McNulty et al. 2006; see Curran 2015). All habitat types were significantly different at (minimally) $p = 0.0031$ (Table 14.3).

Using the linear combinations calculated for the CVA, fossil deer specimens from three Eurasian paleontological sites were categorized into one of the four habitat types.

The calcaneal data overwhelmingly indicate open and intermediate open habitats were available in both France and Romania during the Early Pleistocene (Fig. 14.5, Table 14.4, Appendix 14.2). When combined, cervids with open-adapted calcanei make up 57.4% of the assemblages and intermediate open-adapted calcanei comprise a further 34%, for a pooled total of 91.4%. These results are supported by reconstructions from these sites using different proxies (as reviewed in Curran 2015).

There was only one specimen that was classified into the closed habitat category, belonging to *Cervalces gallicus* from

Table 14.3 Reclassification results (by %) and permutation tests for the extant specimens (training set). InterClosed= Intermediate Closed, InterOpen = Intermediate Open

	Closed	InterClosed	InterOpen	Open
Resubstitution				
Closed	92.86	0.0	0.0	7.14
InterClosed	0.0	81.82	9.09	9.09
InterOpen	5.56	11.11	66.67	16.67
Open	0.0	9.38	15.63	75.0
Cross-validation				
Closed	71.43	7.14	14.29	7.14
InterClosed	27.27	45.45	9.09	18.18
InterOpen	5.56	14.81	61.11	18.52
Open	0.0	12.5	18.75	68.75
	InterOpen	InterClosed	Closed	
Permutation tests				
Open	<0.0001	0.0003	<0.0001	
InterOpen	–	0.0014	<0.0001	
InterClosed	–	–	<0.0001	

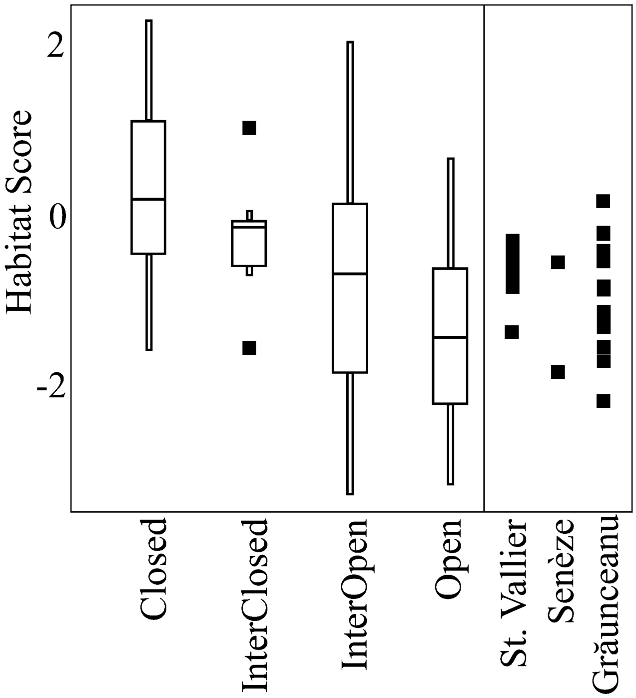

Fig. 14.5 Habitat Score analysis box-and-whiskers diagram. Extant comparative specimens are plotted on the left by habitat type, and specimens from the three fossil sites are plotted on the right. Black horizontal line represents the median, the box encloses the 25th and 75th percentiles, and thin vertical bars (whiskers) include specimens in the range of up to 1.5 times the distance between the quartiles

the French site of Senèze. This species was hypothesized by Breda (2008) to have occupied similar habitats to the modern moose, *Alces alces*, although this was considered contentious as *Cervalces gallicus* had extremely large antlers. The results from this study show that this species had a calcaneus adapted to closed habitats, indicating that there were some forested regions available near the site of Senèze.

A large number of the fossil calcanei in this analysis have not been identified to taxon. While this study is not intended to resolve this, there is an intriguing pattern in the data. When specimen scores for the first canonical variate were regressed against the natural log of centroid size (lnCS), there was a distinct patterning to the distribution of the fossil specimens in this morphospace. Although the R^2 was low (0.092), the p-value indicated significance ($p < 0.0001$). In Figure 14.6A, it can be seen that many of the fossil specimens plot to the negative side on the first canonical variate, indicating that their morphology is not closed-adapted. When the fossil specimen distribution is examined without the extant training set, two or three groups of specimens are evident. In Figure 14.6B, the asterisks are fossil specimens that are assigned only to Cervidae. In this distribution, there is a clear *Eucladoceros* group and a *Croizetoceros* group. Near each are several specimens of unknown taxon and then a group of specimens that falls in between the two groups (larger asterisks). It is possible that the larger specimens belong to *Eucladoceros*, that the smallest specimens belong to *Croizetoceros*, and possibly that the medium/small-sized group belongs to *Cervus philisi*, which is known from known from both St. Vallier and Senèze, France (Valli 2004a, b; Delson et al. 2006). This hypothesis is supported by the habitat assignments for these specimens (see Appendix 14.2): the large specimens were mainly assigned to intermediate open habitat category, which is mainly comprised of *Eucladoceros*, while the medium/small- and small-sized specimens without taxonomic assignments were only assigned to the open habitat category, as were the *Croizetoceros* specimens.

It should be noted that the Dmanisi faunal assemblage contains members of the genus *Eucladoceros*, which were assigned to a more closed habitat (Lordkipanidze et al. 2007, Supplementary Information), however, the analysis here and elsewhere (see especially Curran 2015) indicate a more open-adapted signal for their post-cranial morphology. Although it is likely that several habitat types were available at Dmanisi, there is a substantial grassland signal from palynological records at the time of hominin occupation (Messager et al. 2010a). Coupled with the reconstructions of relatively

Table 14.4 Fossil specimen habitat assignments

Site		Open	InterOpen	InterClosed	Closed
Grăunceanu	*n*	9	5	3	0
	(%)	52.9	29.4	17.6	0
St. Vallier	*n*	14	8	0	0
	(%)	63.6	36.4	0	0
Senèze	*n*	4	3	0	1
	(%)	50	37.5	0	12.5
Totals	*n*	27	16	3	1
	(%)	57.4	34	6.4	2.1

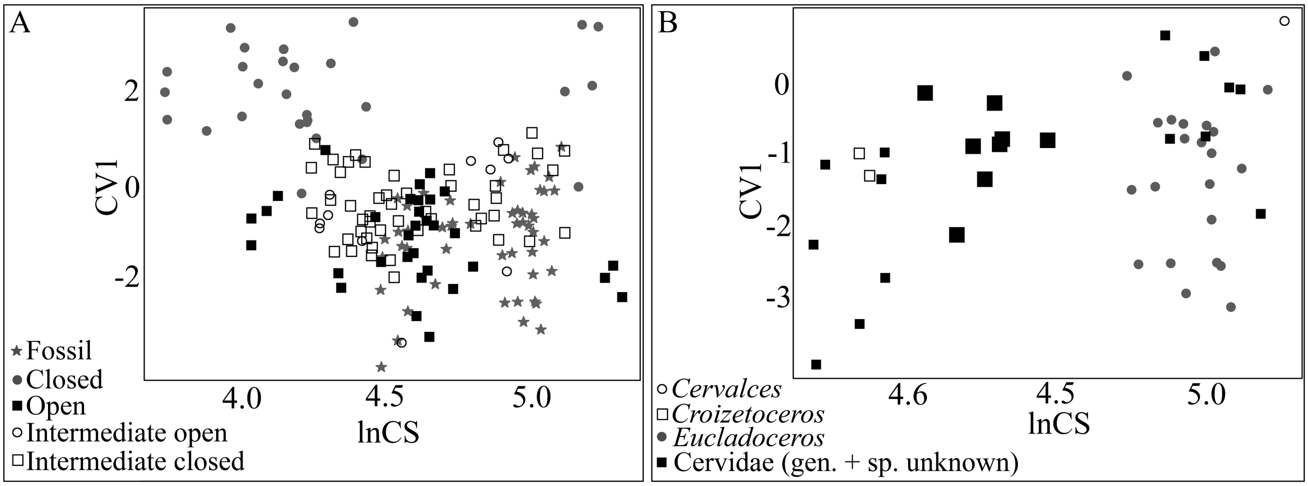

Fig. 14.6 A, Specimens plotted in a morphospace of canonical variate one (CV1) versus the natural log of centroid size (lnCS). B, Only the fossil specimens in the analysis

open habitats and similarity of taxa between Dmanisi and the three European sites examined here, open to intermediate open paleohabitats were likely available across Eurasia at the time of *Homo erectus*'s first arrival there. It is yet to be seen if hominins with similar dates to Dmanisi will also be found in Europe, for there does not seem to have been an ecological or geographic barrier to European dispersal (Moncel 2010).

Future Prospects

In 1993, Rohlf and Marcus declared geometric morphometrics "a revolution in morphometrics" (p. 129). Ten years later, Adams et al. (2004, p. 15) wrote, "We anticipate that over the next few years the geometric morphometric methods that were developed to address shortcomings of what was then the traditional approach to shape analysis will themselves evolve into a standard research protocol … perhaps even becoming the new "traditional" morphometrics". At this point, thirteen years later, in many fields (anthropology, biology, forensics, paleontology, mammalogy, zoology, etc.), geometric morphometrics is nearing the standard method for shape analysis. This is evidenced in the dramatic growth of publications using GM over the last fifteen years (Fig. 14.7, an update to Adams et al. 2004), a

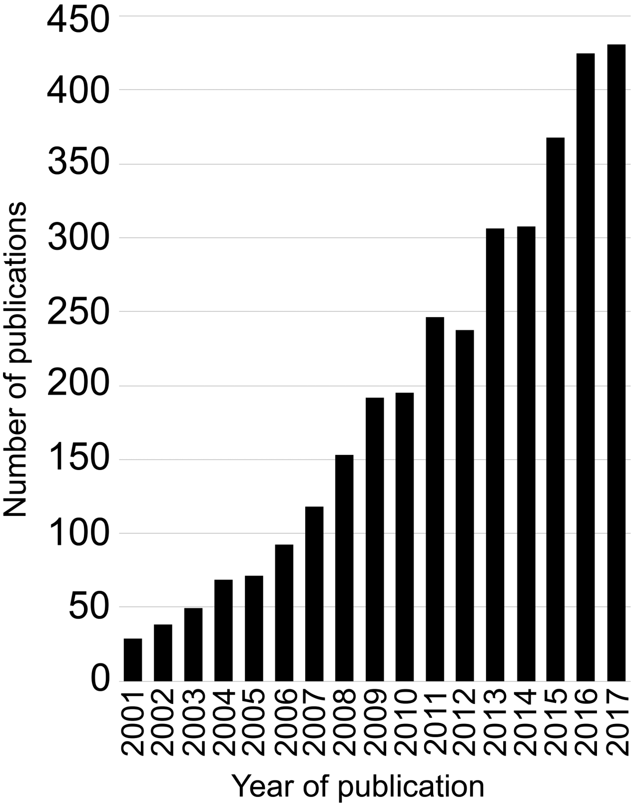

Fig. 14.7 Number of publications that appear in the ISI: Web of Science database per year with a "geometric morphometrics" keyword search

large increase in the number of courses and workshops being offered at universities, professional meetings, and as stand-alone entities (see the Stony Brook morphometrics page at http://life.bio.sunysb.edu/morph/notices.html for a listing of some of these), and the availability of on-line databases such as MorphoSource (Copes et al. 2016), MorphoBrowser (Evans et al. 2007), and others (see Davies et al. 2017). These databases are of special importance, as they make data widely available, storable, and in some cases, reduce issues of inter-observer error (von Cramon-Taubadel et al. 2007; Robinson and Terhune 2017; Shearer et al. 2017).

Greater accessibility to GM data and instruction coupled with open access software, the availability of photogrammetry (Evin et al. 2016), and the decreasing cost of 3D digitizers is partially responsible for the proliferation of GM studies. Equally responsible for the rise in GM's usage are the practitioners of the methods itself. Although GM can be considered a "mature" (Slice 2007, p. 273) method, its base assumptions and applications are constantly being revised (Adams et al. 2013; Bookstein 2017a, b). Recently, methods have been presented for the integration of GM with functional morphology (Bookstein 2015), finite elements analysis (Parr et al. 2012; O'Higgins and Milne 2013; Smith et al. 2015), and genetics (Sherwood and McNulty 2011; Bo et al. 2014; Geiger et al. 2016; Martinez-Abadias et al. 2016). Great strides are also being made in the virtual reconstruction and corrections to deformation of fossil specimens (Gunz et al. 2009; Tallman et al. 2014; Bauer and Harvati 2015; Millella et al. 2015), visualization of shape differences (Klingenberg 2013), and the automation of data collection (Boyer et al. 2011, 2015; Gonzalez et al. 2016). There is no doubt that GM methods will continue to be improved and be integrated further into studies of shape.

In the end, it can be said that GM has great intuitive appeal to researchers interested in shape analysis. There is a certain romantic quality to its mathematics and analysis technique. Thin-plate splines and wire-frame models elegantly display differences in shapes that can be described qualitatively, yet GM data allow for statistical analyses that are not possible with qualitative descriptors. With GM, we can not only quantify shape differences that hitherto may have been described only qualitatively, we can go beyond that and virtually create shapes in a manner that was not previously possible. It is no wonder then that GM has become a standard in the tool kit of morphologists.

Acknowledgements Special thanks to Darin Croft, Scott Simpson, and Denise Su for organizing the excellent "Latest Methods in Cenozoic Paleoecology" symposium and to the Cleveland Museum of Natural History for hosting the event. Funding for this research was provided by National Science Foundation Doctoral Dissertation Improvement Grant BCS-0824607, University of Minnesota Doctoral Dissertation Fellowship, University of Minnesota Herb E. Wright Fellowship in Paleoecology, and University of Minnesota, Department of Anthropology Block Grants. For access to and assistance with collections I thank Alexandru Petculescu (Institute of Speleology, Bucharest, Romania), Aurelian Popescu (Museum of Oltenia, Craiova, Romania), Abel Prieur (Collections de Geologie, Universite C. Bernard Lyon 1, France), Didier Berthet (Collection du Musee des Confluences, Lyon, France), Michi Schulenberg (Chicago Field Museum, USA), Eileen Westwig (American Museum of Natural History, USA), Linda Gordon (National Museum of Natural History, USA), and Chris Conroy (UC Berkeley Museum of Vertebrate Zoology, USA). Thanks to Adam Sylvester for the femoral head visualization in Fig. 14.1 and to the editors and reviewers whose insights greatly improved this manuscript.

Appendix 14.1

Software Packages

Edgewarp: http://brainmap.stat.washington.edu/edgewarp//
EVAN Toolbox: http://evan-society.org/node/42
geomorph (R package): https://cran.r-project.org/web/packages/geomorph/index.html
Landmark editor: http://graphics.idav.ucdavis.edu/research/EvoMorph
MorphoJ: http://www.flywings.org.uk/MorphoJ_page.htm
Morpho (R package): https://cran.r-project.org/web/packages/Morpho/index.html
Morphologika2: https://sites.google.com/site/hymsfme/downloadmorphologica
PAST: http://folk.uio.no/ohammer/past/
R: http://www.r-project.org/

On-line Resources

MorphoBrowser: http://pantodon.science.helsinki.fi/mor phobrowser/
MorphoSource: http://morphosource.org/
Stony Brook Morphometrics page: http://life.bio.sunysb.edu/morph/

Appendix 14.2

ID	Species	Site	Assigned Habitat	Closed	InterClosed	InterOpen	Open
FR684a	Cervidae (m)	Senèze	Open	0.0096	0.0792	0.0839	0.8273
FR684b	Cervidae (m)	Senèze	Open	0.0091	0.1811	0.0838	0.726
FR684c	Cervidae (m)	Senèze	Open	0.0439	0.1076	0.1281	0.7204
FR683a	Cervidae (m)	Senèze	Open	0.0022	0.1576	0.2168	0.6235
FR662a	Cervus (l)	Senèze	InterOpen	0.0094	0.0248	0.5111	0.4547
FR608a	Eucladoceros senezensis	Senèze	InterOpen	0.0938	0.036	0.6379	0.2323
FR574a	Eucladoceros senezensis	Senèze	InterOpen	0.0037	0.001	0.9376	0.0577
FR537a	Alces (Libralces)	Senèze	Closed	0.5834	0.0318	0.1544	0.2305
FR2817	Cervidae (s)	St. Vallier	Open	0	0.0015	0.0013	0.9972
FR2821	Cervidae (s)	St. Vallier	Open	0	0.0021	0.0025	0.9954
FR2816	Cervidae (s)	St. Vallier	Open	0	0.0063	0.0112	0.9825
FR2819	Cervidae (s)	St. Vallier	Open	0.001	0.002	0.0212	0.9758
FR2818	Cervidae (s)	St. Vallier	Open	0.0001	0.0254	0.0189	0.9556
FR2791	Cervidae (l)	St. Vallier	Open	0.0004	0.0157	0.1087	0.8752
FR2808	Cervidae (m)	St. Vallier	Open	0.0067	0.03	0.0906	0.8727
FR2810	Cervidae (s)	St. Vallier	Open	0.0052	0.0199	0.1021	0.8727
FR2805	Cervidae (m)	St. Vallier	Open	0.0002	0.0995	0.1293	0.771
FR2813	Cervidae (s)	St. Vallier	Open	0.0036	0.0231	0.2835	0.6898
FR497716	Croizetoceros ramosus	St. Vallier	Open	0.0025	0.0437	0.2825	0.6713
FR2823	Cervidae (m)	St. Vallier	Open	0.0085	0.0337	0.3265	0.6314
FR2809	Cervidae (m)	St. Vallier	Open	0.0627	0.2448	0.137	0.5555
FR497661	Croizetoceros ramosus	St. Vallier	Open	0.005	0.0068	0.4675	0.5207
FR2130	Eucladoceros senezensis	St. Vallier	InterOpen	0.0096	0.0123	0.696	0.2821
FR2120	Eucladoceros senezensis	St. Vallier	InterOpen	0.0021	0.0123	0.7241	0.2616
FR2792	Cervidae (l)	St. Vallier	InterOpen	0.0053	0.0051	0.8284	0.1612
FR2796	Cervidae (l)	St. Vallier	InterOpen	0.1394	0.0171	0.7031	0.1405
FR2131	Eucladoceros senezensis	St. Vallier	InterOpen	0.1063	0.0043	0.8121	0.0772
FR2795	Cervidae (l)	St. Vallier	InterOpen	0.0288	0.0193	0.878	0.0739
FR2797	Cervidae (l)	St. Vallier	InterOpen	0.0221	0.0124	0.9081	0.0575
FR2798	Cervidae (l)	St. Vallier	InterOpen	0.0267	0.0004	0.9689	0.004
ROIV-V.1	Eucladoceros sp.	Grăunceanu	Open	0	0.017	0.0187	0.9642

References

Adams, D. C. (2011). Quantitative genetics and evolution of head shape in *Plethodon* salamanders. *Evolutionary Biology, 38,* 278–286.

Adams, D. C., Rohlf, F. J., & Slice, D. E. (2004). Geometric morphometrics: ten years of progress following the 'revolution'. *Italian Journal of Morphology, 71,* 5–16.

Adams, D. C., & Otárola-Castillo, E. (2013). Package 'geomorph': geometric morphometric analysis of 2d/3d landmark data. R package version 1.0.

Adams, D. C., Rohlf, F. J., & Slice, D. E. (2013). A field comes of age: geometric morphometrics in the 21st century. *Hystrix: The Italian Journal of Mammology, 24,* 7–14.

Adams, D. C., & Collyer, M. L. (2015). Permutation tests for phylogenetic comparative analyses of high-dimensional shape data: what you shuffle matters. *Evolution, 69,* 823–829.

Aguilar-Medrano, R. (2017). Ecomorphology and evolution of the pharyngeal apparatus of benethic damselfish (Pomacentridae, subfamily Stegastinae). *Marine Biology, 164,* 21.

Arias-Martorell, J., Tallman, M., Potau, J. M., Bello-Hellegouarch, G., & Pérez- Pérez, A. (2015). Shape analysis of the proximal humerus in orthograde and semi-orthograde primates: correlates of suspensory behavior. *American Journal of Primatology, 77,* 1–19.

Arnold, C., Matthews, L. J., & Nunn, C. L. (2012). The 10k trees website: a new online resource for primate phylogeny. *Evolutionary Anthropology, 19,* 114–118.

Baab, K. L., McNulty, K. P., & Rohlf, F. J. (2012). The shape of human evolution: a geometric morphometrics perspective. *Evolutionary Anthropology, 21,* 151–165.

Barr, W. A. (2014). Functional morphology of the bovid astragalus in relation to habitat: controlling phylogenetic signal in ecomorphology. *Journal of Morphology, 275,* 1201–1216.

Barr, W. A. (2015). Paleoenvironments of the Shungura Formation (Plio-Pleistocene: Ethiopia) based on ecomorphology of the bovid astragalus. *Journal of Human Evolution, 88,* 97–107.

Barr, W. A. (2018). Ecomorphology. In D. A. Croft, D. F. Su & S. W. Simpson (Eds.), *Methods in paleoecology: Reconstructing Cenozoic terrestrial environments and ecological communities* (pp. 337–347). Cham: Springer.

Bauer, C. C., & Harvati, K. (2015). A virtual reconstruction and comparative analysis of the KNM-ER 42700 cranium. *Anthropologischer Anzeiger, 72,* 129–140.

Blain, H.-A., Agustí, J., Lordkipanidze, D., Rook, L., & Delfino, M. (2014). Paleoclimatic and paleoenvironmental context of the Early Pleistocene hominins from Dmanisi (Georgia, Lesser Caucasus) inferred from the herpetofaunal assemblage. *Quaternary Science Reviews, 105,* 136–150.

Bo, W., Wang, Z., Xu, F., Fu, G., Sui, Y., Wu, W., et al. (2014). Shape mapping: Genetic mapping meets geometric morphometrics. *Briefings in Bioinformatics, 15,* 571–581.

Bookstein, F. L. (1978). *The measurement of biological shape and shape change* (Lecture Notes in Biomathematics, Vol. 24). New York: Springer-Verlag.

Bookstein, F. L. (1989). Principal warps: thin-plate splines and the decomposition of deformations. *Institute of Electrical and Electronics Engineers, Transactions on Pattern Analysis and Machine Intelligence, 11,* 567–585.

Bookstein, F. L. (1991). *Morphometric tools for landmark data: Geometry and biology*. Cambridge: Cambridge University Press.

Bookstein, F. L. (1996a). Biometrics, biomathematics and the morphometric synthesis. *Bulletin of Mathematical Biology, 58,* 313–365.

Bookstein, F. L. (1996/1997). Landmark methods for forms without landmarks: morphometrics of group differences in outline shape. *Medical Imaging Analysis, 1,* 225–243.

Bookstein, F. L. (2015). The relation between geometric morphometrics and functional morphology, as explored by Procrustes interpretation of individual shape measures pertinent to function. *The Anatomical Record, 298,* 314–327.

Bookstein, F. L. (2016). The inappropriate symmetries of multivariate statistical analysis in geometric morphometrics. *Evolutionary Biology, 43,* 277–313.

Bookstein, F. L. (2017a). A newly noticed formula enforces fundamental limits on geometric morphometric analyses. *Evolutionary Biology, 44,* 522–541.

Bookstein, F. L. (2017b). A method of factor analysis for shape coordinates. *American Journal of Physical Anthropology, 164,* 221–245.

Bookstein, F. L., Chernoff, B., Elder, R., Humphries, J., Smith, G., & Strauss, R. (1985). *Morphometrics in evolutionary biology*. (Special Publication No. 15). Philadelphia: Academy of Natural Sciences.

Bottom-Divet, L., Cornette, R., Houssaye, A., Fabre, A.-C., & Herrel, A. (2017). Swimming and running: a study of the convergence in long bone morphology among semiaquatic mustelids (Carnivora: Mustelidae). *Biological Journal of the Linnean Society, 121,* 38–49.

Boyer, C. B. (1991). *A history of mathematics* (2nd ed.). Hoboken: Wiley.

Boyer, D., Lipman, Y., Clair, E. St., Puente, J., Funkhouser, T., Patel, B., et al. (2011). Algorithms to automatically quantify the geometric similarity of anatomical surfaces. *Proceedings of the National Academy of Sciences, USA, 108,* 18221–18226.

Boyer, D. M., Puente, J., Gladman, J. T., Glynn, C., Mukherjee, S., Yapuncich, G. S., et al. (2015). A new fully automated approach for aligning and comparing shapes. *The Anatomical Record, 298,* 249–276.

Breda, M. (2008). Palaeoecology and palaeoethology of the Plio-Pleistocene genus *Cervalces* (Cervidae, Mammalia) in Eurasia. *Journal of Vertebrate Paleontology, 28,* 886–899.

Cáceres, N., Meloro, C., Carotenuto, F., Passaro, F., Sponchiado, J., Melo, G. L., et al. (2014). Ecogeographical variation in skull shape of capuchin monkeys. *Journal of Biogeography, 41,* 501–512.

Cano, A. R. G., Fernández, M. H., & Álvarez-Sierra, M. Á. (2013). Dietary ecology of Murinae (Muridae, Rodentia): a geometric morphometric approach. *PLoS ONE, 11,* e79080.

Cardini, A., & Elton, S. (2007). Sample size and sampling error in geometric morphometric studies of size and shape. *Zoomorphology, 126,* 121–134.

Cardini, A., & Loy, A. (Eds.). (2013). Virtual morphology and evolutionary morphometrics in the new millennium. *Hystrix: The Italian Journal of Mammology, 24(1).*

Cardini, A., Seetah, K., & Barker, G. (2015). How many specimens do I need? Sampling error in geometric morphometrics: testing the sensitivity of means and variances in simple randomized selection experiments. *Zoomorphology, 134,* 149–163.

Christensen, P. (2008). Evolution of skull and mandible shape in cats (Carnivora: Felidae). *PLoS ONE, 3,* e2807.

Colangelo, P., Castiglia, R., Franchini, P., & Solano, E. (2010). Patterns of shape variation in the eastern African gerbils of the genus *Gerbilliscus*, USA (Rodentia, Muridae): environmental correlations and implications for taxonomy and systematics. *Mammalian Biology, 75,* 302–310.

Cooke, S. B. (2011). Paleodiet of extinct platyrrhines with emphasis on the Caribbean forms: three-dimensional geometric morphometrics of mandibular second molars. *The Anatomical Record, 294,* 2073–2091.

Cooke, S. B., & Terhune, C. E. (2015). Form, function, and geometric morphometrics. *The Anatomical Record, 298,* 5–28.

Copes, L. E., Lucas, L. M., Thostenson, J. O., Hoekstra, H. E., & Boyer, D. M. (2016). A collection of non-human primate computed tomography scans housed in MorphoSource, a repository for 3D data. *Scientific Data, 3,* 160001.

Curran, S. (2009). Hominin paleoecology and cervid ecomorphology. Ph.D. Dissertation, University of Minnesota.

Curran, S. (2012). Expanding ecomorphological methods: geometric morphometric analysis of Cervidae post-crania. *Journal of Archaeological Science, 39,* 1172–1182.

Curran, S. (2015). Examining *Eucladoceros* ecomorphology using geometric morphometrics. *The Anatomical Record, 298,* 291–313.

Curran, S., Terhune, C., Sylvester, A., Gogol, S., & Hubbard, J. (2016). New ecomorphological proxies for paleohabitat reconstructions: Geometric morphometric analyses of cervid joint surface morphology. *PaleoAnthropology Society* meetings, 12 April (2016).

Davies, T. G., Rahman, I. A., Lautenschlager, S., Cunningham, J. A., Asher, R. J., Barrett, P. M., et al. (2017). Open data and digital morphology. *Proceedings of the Royal Society B: Biological Sciences, 284,* 20170194.

DeGusta, D., & Vrba, E. (2003). A method for inferring paleohabitats from the functional morphology of bovid astragali. *Journal of Archaeological Science, 30,* 1009–1022.

DeGusta, D., & Vrba, E. (2005). Methods for inferring paleohabitats from the functional morphology of bovid phalanges. *Journal of Archaeological Science, 32,* 1099–1113.

Delson, E., Faure, M., Guérin, C., Aprile, A., Argant, J., Blackwell, B., et al. (2006). Franco-American renewed research at the Late Villafranchian locality of Senèze (Haute-Loire, France). *Courier Forschunginstitut Senckenberg, 256,* 275–290.

Dunn, R. H. (2018). Functional morphology of the postcranial skeleton. In D. A. Croft, D. F. Su & S. W. Simpson (Eds.), *Methods in paleoecology: Reconstructing Cenozoic terrestrial environments and ecological communities* (pp. 23–36). Cham: Springer.

Dryden, I. L., & Mardia, K. V. (1998). *Statistical shape analysis*. New York: Wiley.

Eronen, J. T., Evans, A. R., Jernvall, J., & Fortelius, M. (2010). The impacts of regional climate on the evolution of mammals: a case study using fossil horses. *Evolution, 64,* 398–408.

Evans, A. R., & Fortelius, M. (2008). Three-dimensional reconstruction of tooth relationships during carnivoran chewing. *Palaeontologia Electronica, 11*(2), 10A.

Evans, A. R., & Pineda-Munoz, S. (2018). Inferring mammal dietary ecology from dental morphology. In D. A. Croft, D. F. Su & S. W. Simpson (Eds.), *Methods in paleoecology: Reconstructing Cenozoic terrestrial environments and ecological communities* (pp. 37–51). Cham: Springer.

Evans, A. R., Wilson, G. P., Fortelius, M., & Jernvall, J. (2007). High-level similarity of dentitions in carnivorans and rodents. *Nature, 445,* 78–81.

Evin, A., Souter, T., Hulme-Beaman, Ameen, C., Allen, R., Viacava, P., et al. (2016). Use of close-range photogrammetry in zooarchaeology: creating accurate 3D models of wolf crania to study dog domestication. *Journal of Archaeological Science: Reports, 9,* 87–93.

Fabre, A.-C., Cornette, R., Goswami, A., & Peigné, S. (2015). Do constraints associated with locomotor habitat drive the evolution of forelimb shape? *Journal of Anatomy, 226,* 596–610.

Falsetti, A. B., Jungers, W. L., & Cole III, T. M. (1993). Morphometrics of the callitrichid forelimb. *International Journal of Primatology, 14,* 551–572.

Fernández, P. J., Holowka, N. B., Demes, B., & Jungers, W. L. (2016). Form and function of the human and chimpanzee forefoot: implications for early hominin bipedalism. *Scientific Reports, 6,* 30532.

Ferring, R., Oms, O., Agusti, J., Berna, F., Niotadze, M., Sheila, T., et al. (2011). Earliest human occupation at Dmanisi (Georgian Caucasus) dated to 1.85–1.78 Ma. *Proceedings of the National Academy of Sciences, USA, 108,* 10432–10436.

Figueirido, B., Palmqvist, P., & Pérez-Claros, J. A. (2005). Ecomorphological correlates of craniodental variation in bears and paleobiological implications for extinct taxa: an approach based on geometric morphometrics. *Journal of Zoology, 277,* 70–80.

Figueirido, B., & Soibelzon, L. H. (2010). Inferring palaeoecology in extinct tremarctine bears (Carnivora, Ursidae) using geometric morphometrics. *Lethaia, 43*, 209–222.

Forrest, F. L., Plummer, T. W., & Raaum, R. L. (2018). Ecomorphological analysis of bovid mandibles from Laetoli Tanzania using 3D geometric morphometrics: implications for hominin paleoenvironmental reconstruction. *Journal of Human Evolution, 114,* 20–34.

Frost, S. R., Marcus, L. F., Bookstein, F. L., Reddy, D. P., & Delson, E. (2003). Cranial allometry, phylogeography, and systematics of large-bodied papionins (Primates: Cercopithecinae) inferred from geometric morphometric analysis of landmark data. *The Anatomical Record, 275A,* 1048–1072.

Furió, M., Agustí, J., Mouskhelishvili, A., Sanisidro, Ó., & Santos-Cubedo, A. (2010). The paleobiology of the extinct venomous shrew *Beremendia* (Sorcidae, Insectivora, Mammalia) in relation to the geology and paleoenvironment of Dmanisi (Early Pleistocene, Georgia). *Journal of Vertebrate Paleontology, 30,* 928–942.

Gabunia, L., Vekua, A., & Lordkipanidze, D. (2000). The environmental contexts of early occupation of Georgia (Transcaucasia). *Journal of Human Evolution, 38,* 785–802.

Gilbert, C., Ropiquet, A., & Hassanin, A. (2006). Mitochondrial and nuclear phylogenies of Cervidae (Mammalia, Ruminantia): systematics, morphology, and biogeography. *Molecular Phylogenetics and Evolution, 40,* 101–117.

Geiger, M. F., Schreiner, C., Delmastro, G. B., & Herder, F. (2016). Combining geometric morphometrics with molecular genetics to investigate a putative hybrid complex: a case study with barbels *Barbus* spp. (Teleostei: Cyprinidae). *Journal of Fish Biology, 88,* 1038–1055.

Gonzalez, P. N., Barbeito-Andres, J., D'Addona, L. A., Bernail, V., & Perez, S. I. (2016). Technical note: Performance of semi and fully automated approaches for registration of 3D surface coordinates in geometric morphometric studies. *American Journal of Physical Anthropology, 160,* 169–178.

Green, J. L., & Croft, D. A. (2018). Using dental mesowear and microwear for dietary inference: a review of current techniques and applications. In D. A. Croft, D. F. Su & S. W. Simpson (Eds.), *Methods in paleoecology: Reconstructing Cenozoic terrestrial environments and ecological communities* (pp. 53–73). Cham: Springer.

Gunz, P., Mitteroecker, P., & Bookstein, F. L. (2005). Semilandmarks in three dimensions. In D. E. Slice (Ed.), *Modern morphometrics in physical anthropology* (pp. 73–98). New York: Kluwer Academic/Plenum Publishers.

Gunz, P., & Mitteroecker, P. (2013). Semilandmarks: a method for quantifying curves and surfaces. *Hystrix: The Italian Journal of Mammology, 24,* 103–109.

Gunz, P., Mitteroecker, P., Neubauer, S., Weber, G. W., & Bookstein, F. L. (2009). Principles for the virtual reconstruction of hominin crania. *Journal of Human Evolution, 57*, 48–62.

Gunz, P., Ramsier, M., Kuhrig, M., Hublin, J.-J., & Spoor, F. (2012). The mammalian bony labyrinth reconsidered, introducing a comprehensive geometric morphometric approach. *Journal of Anatomy, 220,* 529–543.

Hammer, Ø., Harper, D. A. T., & Ryan, P. D. (2001). PAST: Paleontological statistics software package for education and data analysis. *Palaeontologia Electronica, 4*(1:4), 9 pp.

Harcourt-Smith, W. E., Tallman, M., Frost, S. R., Wiley, D. F., Rohlf, F. J., & Delson, E. (2008). Analysis of selected hominoid joint surfaces using laser scanning and geometric morphometrics: a preliminary report. In E. J. Sargis & M. Dagosto (Eds.), *Mammalian evolutionary morphology: A tribute to Frederick S. Szalay* (pp. 373–383). Berlin: Springer Science + Business Media.

Hemmer, H., Kahlke, R.-D., & Vekua, A. (2011). A cheetah *Acinonyx pardinesis* (Croizet et Jobert, 1828) s.l. at the hominin site of Dmanisi (Georgia) – A potential prime meat supplier in Early Pleistocene ecosystems. *Quaternary Science Reviews, 30,* 2703–2714.

Hildebrand, M. (1985). Walking and running. In M. Hildebrand, D. M. Bramble, K. F. Liem, & D. B. Wake (Eds.), *Functional vertebrate morphology* (pp. 38–57). Cambridge, MA, USA: Belknap Press.

Jungers, W. L., Falsetti, A. B., & Wall, C. E. (1995). Shape, relative size, and size-adjustments in morphometrics. *Yearbook of Physical Anthropology, 38,* 137–161.

Kappelman, J. (1988). Morphology and locomotor adaptations of the bovid femur in relation to habitat. *Journal of Morphology, 198,* 119–130.

Kappelman, J. (1991). The paleoenvironment of *Kenyapithecus* at Fort Ternan. *Journal of Human Evolution, 20,* 95–129.

Kaliontzopoulou, A. (2011). Geometric morphometrics in herpetology: modern tools for enhancing the study of morphological variation in amphibians and reptiles. *Basic and Applied Herpetology, 25,* 5–32.

Kendall, D. G. (1977). The diffusion of shape. *Advances in Applied Probability, 9,* 428–430.

Klingenberg, C. P. (2011). MorphoJ: an integrated software package for geometric morphometrics. *Molecular Ecology Resources, 11,* 353–357.

Klingenberg, C. P. (2013). Visualizations in geometric morphometrics: how to read and how to make graphs showing shape changes. *Hystrix, the Italian Journal of Mammalogy, 24,* 15–24.

Klingenberg, C. P. (2016). Size, shape, and form: concepts of allometry in geometric morphometrics. *Development, Genes, and Evolution, 226,* 113–137.

Kovarovic, K., & Andrews, P. (2007). Bovid post-cranial ecomorphological survey of the Laetoli paleoenvironment. *Journal of Human Evolution, 52,* 663–680.

Kovarovic, K., Aiella, L. C., Cardini, A., & Lockwood, C. A. (2011). Discriminant function analyses in archaeology: are classification rates too good to be true? *Journal of Archaeological Science, 38,* 3006–3018.

Lordkipanidze, D., Jashashvili, T., Vekua, A., De León, M. S. P., Zollikofer, C. P., Rightmire, G. P., et al. (2007). Postcranial evidence from early *Homo* from Dmanisi, Georgia. *Nature, 449,* 305–310.

MacLeod, N. (1999). Generalizing and extending the eigenshape method of shape space visualization and analysis. *Paleobiology, 25,* 107–138.

Mander, L., & Punyasena, S. W. (2018). Fossil pollen and spores in paleoecology. In D. A. Croft, D. F. Su & S. W. Simpson (Eds.), *Methods in paleoecology: Reconstructing Cenozoic terrestrial environments and ecological communities* (pp. 213–232). Cham: Springer.

Marcus, L. F., Bello, E., & García-Valdecasas, A. (Eds.). (1993). *Contribution to morphometrics*. Madrid: Monografias del Museo Nacional de Ciencias Naturales.

Marcus, L. F., Corti, M., Loy, A., Naylor, G. J. P., & Slice, D. E. (Eds.). (1996). *Advances in morphometrics*. (NATO ASI Series A: Life Sciences, Vol. 284). New York: Plenum.

Martinez-Abadias, N., Mateu, R., Niksic, M., Russo, L., & Sharpe, J. (2016). Geometric morphometrics on gene expression patterns within phenotypes: a case study on limb development. *Systematic Biology, 65,* 194–211.

McGuire, J. L. (2010). Geometric morphometrics of vole (*Microtus californicus*) dentition as a new paleoclimate proxy: shape change along geographic and climatic clines. *Quaternary International, 212,* 198–205.

McNulty, K. P. (2003). *Geometric morphometric analyses of extant and fossil hominoid craniofacial morphology*. Ph.D. Dissertation, City University of New York.

McNulty, K. P., Frost, S. R., & Strait, D. S. (2006). Examining affinities of the Taung child by developmental simulation. *Journal of Human Evolution, 51,* 274–296.

McNulty, K. P., & Vinyard, C. J. (2015). Morphometry, geometry, function and the future. *The Anatomical Record, 298,* 328–333.

Meloro, C., Cáceres, N., Carotenuto, F., Passaro, F., Sponchiado, J., Melo, G. L., et al. (2014). Ecogeographical variation in skull morphometry of howler monkeys (Primates: Atelidae). *Zoologischer Anzeiger, 253,* 345–359.

Messager, E., Lordkipanidze, D., Kvavadze, E., Ferring, C. R., & Voinchet, P. (2010a). Palaeoenvironmental reconstruction of Dmanisi site (Georgia) based on palaeobotanical data. *Quaternary International, 223–224,* 20–27.

Messager, E., Lordkipanidze, D., Delhon, C., & Ferring, C. R. (2010b). Palaeoecological implications of the Lower Pleistocene phytolith record from the Dmanisi Site (Georgia). *Palaeogeography, Palaeoclimatology, Palaeoecology, 288,* 1–13.

Millella, M., Zollikofer, C. P. E., & Ponce de León, M. S. (2015). Virtual reconstruction and geometric morphometrics as tools for paleopathology: a new approach to study rare developmental disorders of the skeleton. *The Anatomical Record, 298*, 335–345.

Mitteroecker, P., & Bookstein, F. (2011). Linear discrimination, ordination, and the visualization of selection gradients in modern morphometrics. *Evolutionary Biology, 38*, 100–114.

Mitteroecker, P., & Gunz, P. (2009). Advances in geometric morphometrics. *Evolutionary Biology, 36,* 235–247.

Moncel, M.-H. (2010). Oldest human expansions in Eurasia: favoring and limiting factors. *Quaternary International, 223–224,* 1–9.

Monteiro, L. R. (1999). Multivariate regression models and geometric morphometrics: the search for causal factors in the analysis of shape. *Systematic Biology, 48,* 192–199.

Monteiro, L. R., Duarte, L. C., & dos Reis, S. F. (2003). Environmental correlates of geographical variation in skull and mandible shape of the punar´e rat *Thrichomys apereoides* (Rodentia: Echimyidae). *Journal of Zoology, London, 261,* 47–57.

Morgan, C. C., & Álvarez, A. (2012). The humerus of South American caviomorph rodents: shape, function and size in a phylogenetic context. *Journal of Zoology, 290,* 107–116.

Muñoz, N. A., Cassini, G. H., Candela, A. M., & Vizcaíno, S. F. (2017). Ulnar articular surface 3D landmarks and ecomorphology of small mammals: a case study of two early Miocene typotheres (Notoungulata) from Patagonia. *Earth and Environmental Science Transactions of the Royal Society of Edinburgh, 106,* 315–323.

Neff, N. A., & Marcus, L. F. (1980). *A survey of multivariate methods for systematics*. New York: American Museum of Natural History.

Nowak, R. (1999). *Walker's mammals of the world,* (Vol. II, pp. 1091–1133). Baltimore: John Hopkins University Press.

Nomade, S., Pastre, J. F., Guillou, H., Faure, M., Guérin, C., Delson, E., et al. (2014). ^{40}Ar/^{39}Ar constraints on some French landmark Late Pliocene to Early Pleistocene large mammalian paleofaunas: paleoenvironmental and paleoecological implications. *Quaternary Geochronology, 21,* 2–15.

O'Higgins, P., & Jones, N. (2006). Tools for statistical shape analysis. Hull York Medical School. http://hyms.fme.googlepages.com/resources.

O'Higgins, P., & Milne, N. (2013). Applying geometric morphometrics to compare changes in size and shape arising from finite element analyses. *Hystrix, the Italian Journal of Morphology, 24,* 126–132.

Palmqvist, P. (2002). On the community structure of the large mammals assemblage from Dmanisi (East Georgia, Caucasus). In M. D. Renzi, M. V. P. Alonso, M. Belinchón, E. Penalver, P. Montoya & A. Márquez-Aliaga (Eds.), *Current topics in taphonomy and fossilization* (pp. 361–383). Valencia: Ayuntamentio de Valencia.

Panagiotopoulou, O. (2009). Finite element analysis (FEA): applying an engineering method to functional morphology in anthropology and human biology. *Annals of Human Biology, 36,* 609–623.

Parr, W. C. H., Wroe, S., Chamoli, U., Richards, H. S., McCurry, M. R., Clausen, P. D., et al. (2012). Toward integration of geometric morphometrics and computational biomechanics: new methods for 3D virtual reconstruction and quantitative analysis of Finite Element Models. *Journal of Theoretical Biology, 301,* 1–14.

Peppe, D. J., Baumgartner, A., Flynn, A., & Blonder, B. (2018). Reconstructing paleoclimate and paleoecology using fossil leaves. In D. A. Croft, D. F. Su & S. W. Simpson (Eds.), *Methods in paleoecology: Reconstructing Cenozoic terrestrial environments and ecological communities* (pp. 287–315). Cham: Springer.

Perez, S. I., Bernal, V., & Gonzalez, P. N. (2006). Differences between sliding semi-landmark methods in geometric morphometrics, with an application to human craniofacial and dental variation. *Journal of Anatomy, 208,* 769–784.

Piras, P., Marcolini, F., Claude, J., Venture, J., Kotsakis, T., & Cubo, J. (2012). Ecological and functional correlates of molar shape variation in European populations of *Arvicola* (Arvicolinae, Rodentia). *Zoologischer Anzeiger, 251,* 335–343.

Plummer, T. W., & Bishop, L. C. (1994). Hominid paleoecology at Olduvai Gorge, Tanzania as indicated by antelope remains. *Journal of Human Evolution, 27,* 47–75.

Plummer, T. W., Bishop, L. C., & Hertel, F. (2008). Habitat preference of extant African bovids based on astragalus morphology: operationalizing ecomorphology for palaeoenvironmental reconstruction. *Journal of Archaeological Science, 35,* 3016–3027.

Plummer, T. W., Ferraro, J. V., Louys, J., Hertel, F., Alemseged, Z., Bobe, R., et al. (2015). Bovid ecomorphology and hominin paleoenvironments of the Shungura Formation, lower Omo River Valley, Ethiopia. *Journal of Human Evolution, 88,* 108–126.

Raia, P. (2004). Morphological correlates of tough food consumption in large land carnivores. *Italian Journal of Zoology, 71,* 45–50.

Renaud, S., Dufour, A.-B., Hardouin, E. A., Ledevine, R., & Auffray, J.-C. (2015). Once upon multivariate analyses: when they tell several stories about biological evolution. *PLoS ONE, 10,* e0132801.

Ritzman, T. B., Terhune, C. E., Gunz, P., & Robinson, C. A. (2016). Mandibular ramus shape of *Australopithecus sediba* suggests a single variable species. *Journal of Human Evolution, 10,* 54–64.

Robinson, C., & Terhune, C. E. (2017). Error in geometric morphometric data collection: combining data from multiple sources. *American Journal of Physical Anthropology, 164,* 62–75.

Rohlf, F. J. (2015). The tps series of software. *Hystrix, the Italian Journal of Mammalogy, 26,* 9–12.

Rohlf, F. J., & Bookstein, F. L. (Eds.). (1990). *Proceedings of the Michigan Morphometrics Workshop.* University of Michigan Museum of Zoology Special Publication 2.

Rohlf, F. J., & Marcus, L. F. (1993). A revolution in morphometrics. *Trends in Ecology & Evolution, 8,* 129–132.

Rohlf, F. J., & Corti, M. (2000). Use of two-block partial least-squares to study covariation in shape. *Systematic Biology, 49,* 740–753.

Schlager, S. (2017). Morpho and Rvcg – Shape analysis in R. In G. Zheng, S. Li & G. Szekely (Eds.), *Statistical shape and deformation analysis* (pp. 217–256). Cambridge: Academic Press.

Scott, R., Kappelman, J., & Kelley, J. (1999). The paleoenvironment of *Sivapithecus parvada*. *Journal of Human Evolution, 36,* 245–274.

Shearer, B. M., Tallman, M., Cooke, S. B., Halenar, L. B., Reber, S. L., Plummer, J., et al. (2017). Evaluating causes of error in landmark-based data collection using scanners. *PLoS ONE, 12,* e0187452.

Sheets, H. D., Covino, K. M., Panasiewicz, J. M., & Morris, S. R. (2006). Comparison of geometric morphometric outline methods in the discrimination of age-related differences in feather shape. *Frontiers in Zoology, 3,* 15.

Sherwood, R. J., & McNulty, K. P. (2011). Dissecting the genetic architecture of craniofacial shape. In P. E. Lestrel (Ed.), *Biological shape analysis: Proceedings of the 1st international symposium* (pp. 145–171). Singapore: World Scientific.

Slater, G. J., Figuerirido, B., Louis, L., Yang, P., & Van Valkenburgh, B. (2010). Biomechanical consequences of rapid evolution in the polar bear linage. *PLoS ONE, 5,* e13870.

Slice, D. E. (2002). Morpheus et al. Department of Ecology and Evolution. State University of New York, Stony Brook.

Slice, D. E. (2005). Modern morphometrics. In D. E. Slice (Ed.), *Modern morphometrics in physical anthropology* (pp. 1–45). New York: Kluwer Academic/Plenum Publishers.

Slice, D. E. (2007). Geometric morphometrics. *Annual Review of Anthropology, 36,* 261–281.

Smith, A. L., Benazzi, S., Ledogar, J. A., Tamvada, K., Smith, L. C. P., Weber, G. W., et al. (2015). Biomechanical implications of intraspecific shape variation in chimpanzee crania: moving toward an integration of geometric morphometrics and finite element analysis. *The Anatomical Record, 298,* 122–144.

Smits, P. D., & Evans, A. R. (2012). Functional constraints on tooth morphology in carnivorous mammals. *BMC Evolutionary Biology, 12,* 146.

Sommer III, H. J., Eckhardt, R. B., & Shiang, T. Y. (2006). Superquadratic modeling of cranial and cerebral shape and asymmetry. *American Journal of Physical Anthropology, 129,* 189–195.

Strömberg, C. A. E., Dunn, R. E., Crifò, C., & Harris, E. B. (2018). Phytoliths in paleoecology: analytical considerations, current use, and future directions. In D. A. Croft, D. F. Su & S. W. Simpson (Eds.), *Methods in paleoecology: Reconstructing Cenozoic terrestrial environments and ecological communities* (pp. 233–285). Cham: Springer.

Tallman, M., Amenta, A., Delson, E., Frost, S. R., Ghosh, D., Klukkert, Z. S., et al. (2014). Evaluation of a new method of fossil retrodeformation by algorithmic symmetrization: crania of papionins (Primates: Cercopithecidae) as a test case. *PLoS ONE, 9,* e100833.

Tappen, M. J., Lordkipanidze, D., Bukshianidze, M., Vekua, A., & Ferring, R. (2007). Are you in or out (of Africa)? In T. R. Pickering, K. Schick, & N. Toth (Eds.), *Breathing life into fossils: Taphonomic studies in honor of C. K. Brain* (pp. 119–135). Bloomington: Stone Age Institute Press.

Taylor, A. C., Lautenschlager, S., Qi, Z., & Rayfield, E. J. (2016). Biomechanical evaluation of different musculoskeletal arrangements in *Psittacosaurus* and implications for cranial function. *The Anatomical Record, 300,* 49–61.

Thompson, D. W. (1917). *On growth and form.* London: Cambridge University Press.

Tocheri, M. W., Solhan, C. R., Orr, C. M., Femiani, J., Frohlich, B., Groves, C. P., et al. (2011). Ecological divergence and medial cuneiform morphology in gorillas. *Journal of Human Evolution, 60,* 171–184.

Tocheri, M. W., Orr, C. M., Jacofsky, M. C., & Marzke, M. W. (2008). The evolutionary history of the hominin hand since the last common ancestor of *Pan* and *Homo*. *Journal of Anatomy, 212,* 544–562.

Valli, A. M. F. (2004a). Cervidae from the late Pleistocene deposit (Mid-Villafranchian) of Saint-Vallier, (Drôme, France). *Geobios, 37*, S191–S232.

Valli, A. M. F. (2004b). Taphonomy of Saint-Vallier (Drôme, France), the reference locality for biozone MN17 (Upper Pliocene). *Lethaia, 37*, 337–350.

van Heteren, A. H., MacLarnon, A., Soligo, C., & Rae, T. C. (2016). Functional morphology of the cave bear (*Ursus spelaeus*) mandible: a 3D geometric morphometric analysis. *Organisms, Diversity & Analysis, 16,* 299–314.

von Cramon-Taubadel, N., Frazier, B. C., & Lahr, M. M. (2007). The problem of assessing landmark error in geometric morphometrics: theory, methods, and modifications. *American Journal of Physical Anthropology, 134,* 24–35.

Walmsley, A., Elton, S., Louys, J., Bishop, L. C., & Meloro, C. (2012). Humeral epiphyseal shape in the Felidae: the influence of phylogeny, allometry, and locomotion. *The Journal of Morphology, 273,* 1424–1438.

Weinand, D. C. (2007). A study of parametric versus non-parametric methods for predicting paleohabitat from Southeast Asia bovid astragali. *Journal of Archaeological Science, 34,* 1774–1783.

White, J. (2009). Geometric morphometric investigation of molar shape diversity in modern lemurs and lorises. *The Anatomical Record, 292,* 701–719.

Wiley, D. F., Amenta, N., Alcantara, D. A., Ghosh, D., Kil, Y. J., Delson, E., Harcourt-Smith, W., Rohlf, F. J., St. John, K., & Hamann, B. (2005). Evolutionary morphing. *IEEE Visualization, Proceedings*, 431–438.

Zelditch, M. L., Swiderski, D. L., Sheets, H. D., & Fink, W. L. (2004). *Geometric morphometrics for biologists: A primer*. London: Elsevier Academic Press.